Proceedings of the
Annual Stability Conference
Structural Stability Research Council
Toronto, Canada, March 25-28, 2014

Web post buckling resistance of longitudinally stiffened plate girders

L.P.Subramanian[1], D.W.White[2]

Abstract
The current AASHTO specification requirements for the web bend buckling factor R_b do not consider the effect of longitudinal stiffeners in developing plate girder web post buckling flexural resistance. This is a deficiency that can have significant impact especially in regions of negative flexural resistance. This paper evaluates the impact of longitudinal stiffeners on the flexural resistance as well as the requirements on longitudinal stiffeners to develop post buckling capacity. The paper discusses test simulations on straight girders with single longitudinal stiffeners. It is found that there can be up to 50% of savings relative to the current conservative estimates in AASHTO in the negative flexural regions under certain conditions by including the effects of longitudinal stiffeners on the girder flexural capacity. The authors study the impact of various parameters on the contribution of longitudinal stiffeners to the plate girder strength.

1. Introduction

Current AASHTO LRFD specifications require the use of longitudinal stiffeners on plate girders when $D/t_w > 150$. The longitudinal stiffeners are designed to prevent web bend buckling during construction and under service load conditions. However, for cases where the web bend buckling strength is exceeded, they are discounted in determining the web post buckling strength. Once the web bend buckles, the portion of the web in compression becomes less effective in carrying additional load, and the stresses are shed largely to the compressive flange of the girder. The stress variation in the web is nonlinear at post buckling stress levels. R_b is a post buckling reduction factor on the flexural strength of the compressive flange that accounts for this load shedding from the web. The tension flange stresses are not significantly impacted by load shedding from the web (Basler and Thurliman, 1961). Also, the provisions ensure that the reduction in compressive flange flexural resistance due to web bend buckling is negligible in composite sections under positive flexure. R_b is a function of the slenderness of the web in compression, and its area relative to the area of the compressive flange. The current equation for R_b in AASHTO is derived principally from the equations developed by Basler and Thurliman (1961) for webs without longitudinal stiffeners. In this paper, the authors perform a suite of studies by means of finite element test simulations in ABAQUS (Simulia, 2013) to assess the effects of various design parameters such as the panel aspect ratio, the width of the compression

[1] Graduate Research Assistant, Georgia Institute of Technology, <pslakshmipriya@gatech.eduu>
[2] Professor, Georgia Institute of Technology, <don.white@ce.gatech.edu>

flange, the web slenderness ratio, the depth of web in compression, and the area and lateral rigidity of the longitudinal stiffener. The current paper is restricted to the study of straight girders with single longitudinal stiffeners located at the theoretical optimum position for restraining web bend buckling.

2. Test Parameters

2.1 Constant parameters

These parameters are kept constant in all the parametric studies presented in this paper

a. The yield stress of all plated elements, F_y is 50ksi.
b. The depth of web panel, D is 150 inches.
c. The depth of the longitudinal stiffener is at d_s/ D_c = 0.4 (theoretical optimum stiffener depth)
d. The transverse stiffeners are designed to meet the AASHTO (2007) minimum requirements.
e. The width-to-thickness ratio, b_l/t_l, of the longitudinal stiffeners is designed to satisfy the AASHTO (2007) maximum limit.

2.2 Loading

The straight girders considered are subjected to four point bending tests; with the test panel subjected to pure bending and flanked by an end fixture on either side. The test fixtures are designed sufficiently to ensure occurrence of the flexural strength limit in the test specimens. The test setup is based upon Cooper's experimental tests (1965). The compression flanges are braced adequately to prevent lateral torsional buckling (LTB) in this study.

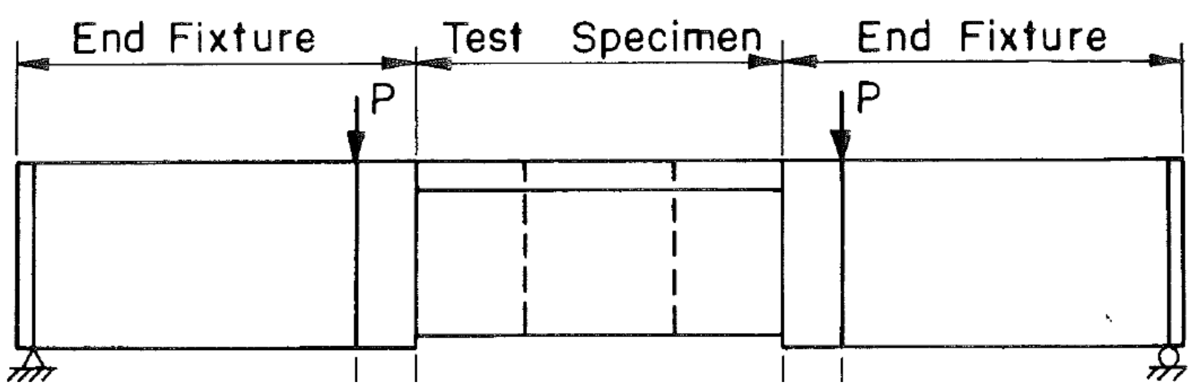

Figure 1: Experimental test set up (Cooper, 1965)

2.3 Variable Parameters

The following parameters are varied in the different studies to assess their impact on the effect of the longitudinal stiffener in contributing to the plate girder strength.

a. D/t_w = 300, 240, 200
b. d_o/D = 0.75,1.0, 1.5, 2.0
c. b_{fc} = D/6, D/5, D/4
d. D_c/D = 0.5, 0.625, 0.75
e. A_l / A_{wc}
f. I_l ,

where:

D_c= depth of web in compression

t_w = thickness of web
d_o = distance between transverse stiffeners
b_{fc} = width of compression flange
A_l = area of cross section of longitudinal stiffener
A_{wc} = area of web in compression
b_l = projecting width of the longitudinal stiffener
t_l = thickness of the longitudinal stiffener
I_l = moment of inertia of the longitudinal stiffener including an effective width of web ($18t_w$) taken about the neutral axis of the combined section
The parameters A_l / A_{wc} and I_l are varied by designing the longitudinal stiffener sizes to meet the minimum requirements as per AASHTO. This is a function of d_o/ D and D/t_w.

3. Residual Stress Pattern

The self-equilibrating residual stress pattern shown in Fig. 2 is based on residual stresses measured by Prawel (1974) in three-plate girder construction without longitudinal stiffeners. They are taken in this work as representative nominal residual stresses for the flange and web plates of general welded I girders.

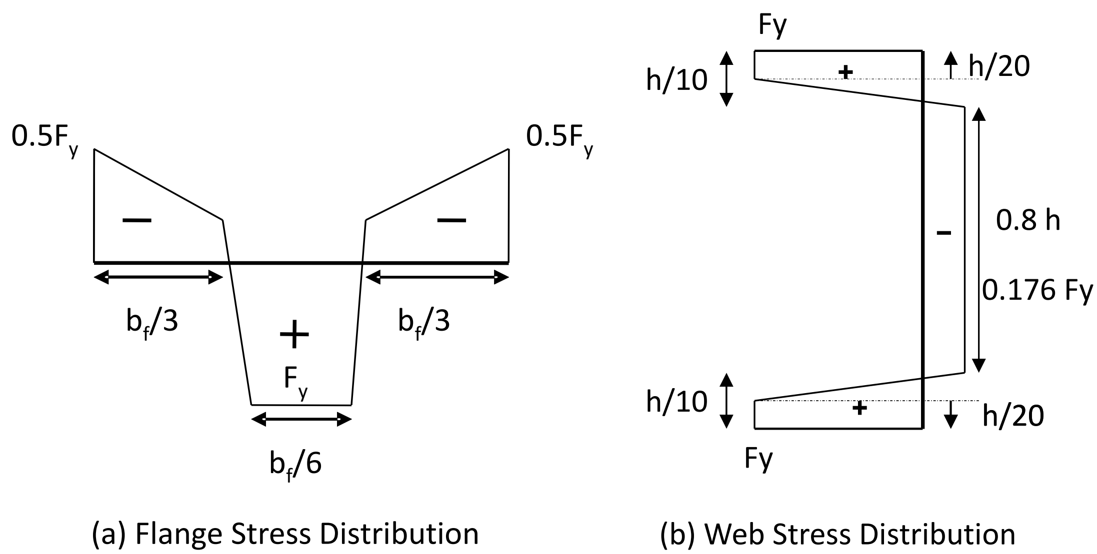

Figure 2: Residual stress distribution (Prawel (1974))

The web compressive residual stress in the above pattern is 0.176 F_y. However, in these studies, this stress is limited to the web buckling stress under uniform longitudinal compression with idealized simply supported edge conditions, which is often a very small fraction of 0.176 F_y. These web residual stresses are limited because the physical web cannot be manufactured to develop residual stresses that significantly exceed this buckling stress. The web residual stresses in the heat affected zone of the web, equal to F_y in the above sketch, are scaled by the ratio of the above approximation of the web buckling stress under uniform longitudinal compression to 0.176 F_y.

A self-equilibrating residual stress pattern in the longitudinal stiffener is developed based on an initial heat affected zone of $b_s/5$. This pattern is shown in Fig. 3. This pattern is obtained by starting with a typical residual stress pattern where the heat-affected zone has a tensile residual stress equal to F_y and the rest of the plate has a self-equilibrating residual compression. The elastic flexural stresses necessary to put this plate in moment equilibrium, i.e., sum of moments about a reference point equal to zero in addition to total sum of longitudinal forces equal to zero, are then added to the above base stresses to create a representative statically admissible residual stress distribution in the longitudinal stiffener.

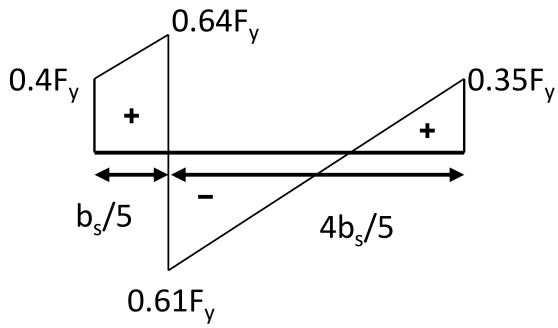

Figure 3: Residual stress distribution in Longitudinal Stiffener

4. Imperfection Patterns and Sensitivity

To determine the most critical geometric imperfection that may be experienced by the test girders, six base imperfection patterns were studied in ABAQUS for the condition of pure bending. The girder dimensions for this study mirror those from test girder LB3 from Cooper's experimental tests (1965). The web is 55 inches x 0.125 inches, and the flanges are 12 inches by 0.75 inches as shown in Table 1.

Table 1: Girders used in imperfection sensitivity studies (all dimensions in inches)

	Web[d]	Comp.Flange[d]	Tens.Flange[d]	Longitudinal Stiffener	Transverse Stiffener	d_s/D	d_o/D
Girder 1	55 x 0.125	12 x 0.75	12 x 0.75	-	3 x 0.25	0.2	1
Girder 2[a]	55 x 0.125	12 x 0.75	12 x 0.75	1.75 x 0.125	3 x 0.25	0.2	1
Girder 3[b]	55 x 0.125	12 x 0.75	12 x 0.75	2.5 x 0.125	3 x 0.25	0.2	1
Girder 4[c]	55 x 0.125	12 x 0.75	12 x 0.75	3.5x0.25	3 x 0.25	0.2	1

a. Cooper's test specimen with the size of longitudinal girder set to meet minimum b/t ratio as per AASHTO
b. Cooper's test specimen (LB3)
c. Same b_l/t_l as Girder 2, but with four times the cross section area of the longitudinal stiffener. .
d. Yield stress of flange = 37ksi, web = 34 ksi.

The imperfection patterns shown in Fig. 4 are used as the base imperfection patterns for the imperfection sensitivity studies. The test simulations are first run using these base imperfection patterns and the limit load and failure mode (i.e., the lateral deflected shape of the girder web at the limit load) is determined from these analyses. The girder deflection at the limit load, which defines the failure mode, is then scaled appropriately as described below to use as the actual imperfection for the final test simulation analysis. In other words, the test simulation analysis is run twice; once with the base imperfection patterns shown in Fig. 4 as the initial geometric imperfection, and a second time by using the failure mode, scaled to satisfy AWS (2010) tolerances on the maximum web out-of-flatness, as the initial imperfection. In the imperfection sensitivity analyses discussed below, this process is repeated a third time, by using the failure mode from the second analysis, and again scaling it as an imperfection for the third run. It is observed that the failure mode and the limit load do not change significantly by running the analysis a third time. Therefore, the models are only analyzed through steps one and two above for the subsequent parametric studies discussed in this paper. This relatively elaborate procedure appears to identify approximately worst-case geometric imperfections in terms of the corresponding effective "true R_b" of the test girders.

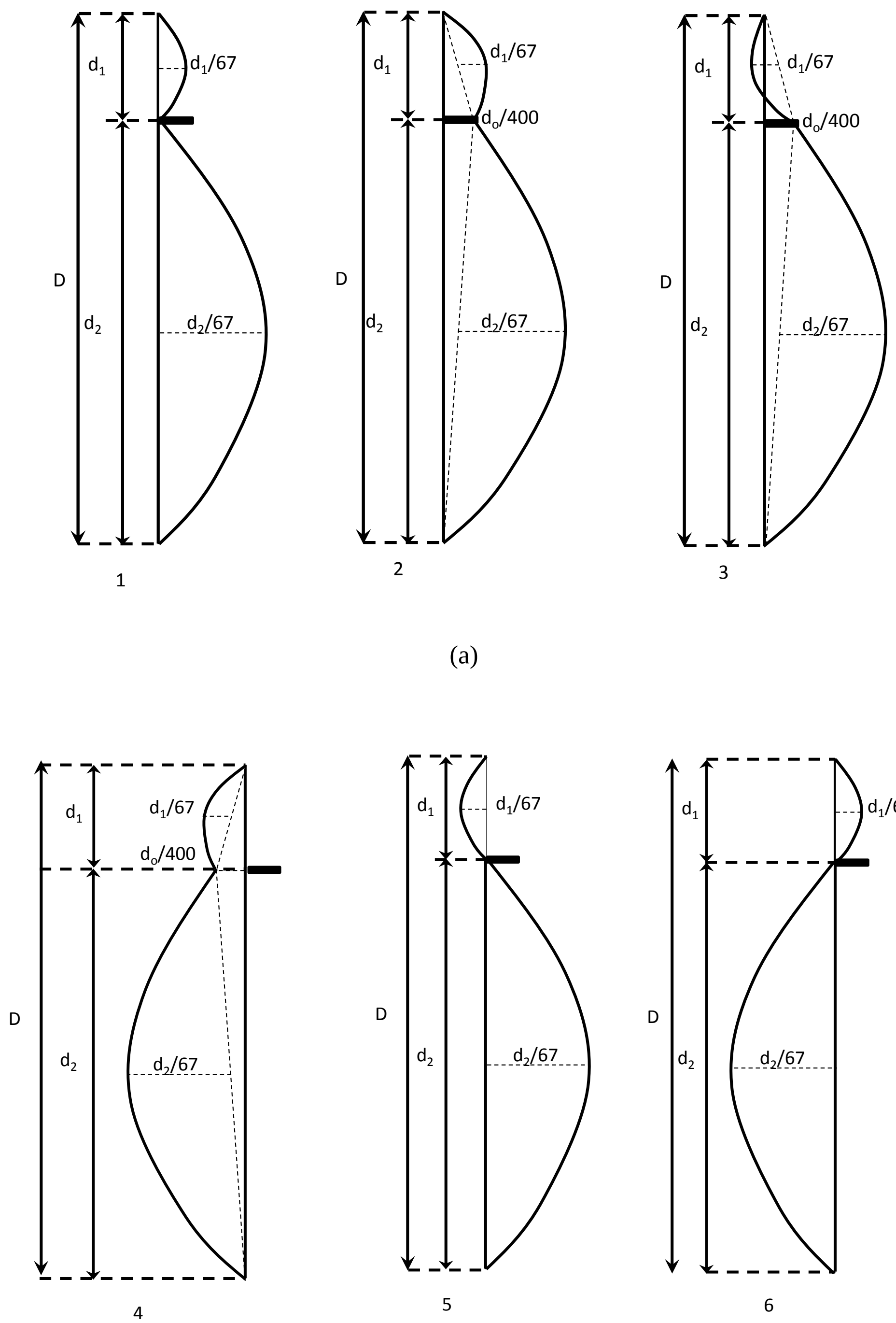

(b)

Figure 4: Base imperfection patterns on web for first analysis

AWS allows a maximum imperfection of 1/67 times the least panel dimension. The imperfection patterns shown in Fig. 4 are also analyzed for an imperfection scale of 1/120 of the least panel dimension in order to assess the sensitivity of the results to the magnitude of the imperfection. The failure modes from the analyses are scaled such that the maximum imperfection on the web panel out of plane is never greater than *D/67*(or *D/120*), while also simultaneously ensuring that the maximum deviation from a straight edge measured in each of the web sub-panels is less than 1/67(or 1/120) times its least panel dimension. The scaled failure mode is then seeded as an initial imperfection for the subsequent analysis. Flange initial imperfections (i.e., flange sweep and flange tilt) are neglected in these studies. The longitudinal stiffeners follow the profile of the web imperfection without any tilt (the web geometric imperfections generally can induce some significant torsional rotation of the longitudinal stiffener).

Fig. 5 (not to scale) shows the failure mode profile at the middle of the test panel after the first analysis using imperfection pattern 2. This is scaled as described above as the imperfection for the final analysis.

The girders in Table 1 have webs with overall slenderness ratios D/t_w of 440, per Cooper's (1965) studies. The imperfection sensitivity studies are also carried out on girders with a web slenderness ratio D/t_w of 300 (maximum allowed as per current AASHTO LRFD provisions) by changing the web thicknesses on girders 1 to 4 in Table 1 to 0.183 inches.
The analyses are performed in ABAQUS using the residual stresses as shown in Figs. 2 and 3, and the initial seed imperfection patterns as shown in Fig. 4. The results reported in Tables 2, 3, and 4 are obtained after scaling the failure modes from successive test simulation analyses twice subsequent to the initial analyses with the imperfection patterns in Fig 4. It is observed that there is no significant difference between the second and third analyses. Hence, in the subsequent parametric studies, the failure modes from a initial test simulation analysis, with the seed imperfection, are scaled only once to set the initial imperfection for the final test simulation solutions. The values reported for Girder 1 (the girder without longitudinal stiffening) are with an initial base imperfection of *D/67* imposed at the center of the web panel.

Tables 2 and 3 and 4 show the R_b values obtained for Girders 1 to 4 with overall web slenderness ratios D/t_w of 440 and maximum imperfection magnitudes of *D/67* and *D/120*. Table 4 shows the R_b values obtained for Girders 1 to 4 with overall web slenderness ratios D/t_w of 300 and a maximum imperfection magnitude of *D/67*. Fig. 6 shows the normal stresses at the mid thickness of the web for Girder 4 with a web slenderness ratio of D/t_w 440 and a maximum imperfection magnitude of *D/67*. Fig. 6 is representative of all the other girders with different slenderness ratios and maximum imperfection magnitudes.

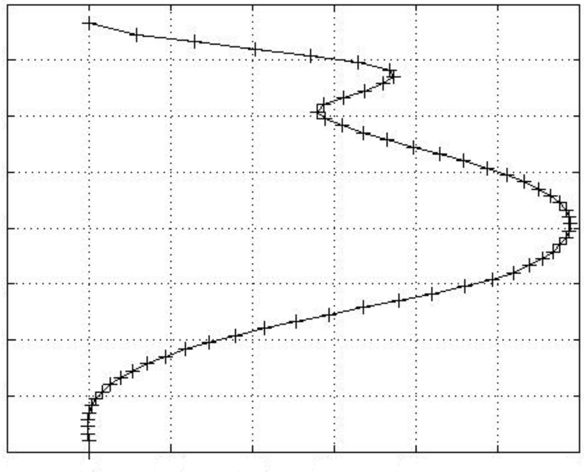

Figure 5: Imperfection pattern on web for second analysis (failure mode from first analysis with imperfection 2)

Table 2: R_b for girders in Table 1 with D/t_w =440

	Imperfection							Difference between Max and Min R_b
	Magnitude	1	2	3	4	5	6	
Girder 1	*D/67*	0.9207						
Girder 2	*D/ 67*	0.9352	0.9356	0.9356	0.9471	0.9363	0.9468	1.2711
Girder 3	*D/ 67*	0.9483	0.9444	0.9455	0.9607	0.9655	0.9534	2.2358
Girder 4	*D/ 67*	1.0066	1.0087	1.0083	1.0012	1.0075	1.0058	0.7486

Table 3: R_b for girders in Table 1 with D/t_w =440

	Imperfection							Difference between Max and Min R_b
	Magnitude	1	2	3	4	5	6	
Girder 1	*D/120*	0.9258						
Girder 2	*D/120*	0.9424	0.9405	0.9416	0.9434	0.9484	0.9429	0.8351
Girder 3	*D/120*	0.9504	0.9530	0.9806	0.9600	0.9680	0.9516	3.1721
Girder 4	*D/120*	0.9839	0.9811	0.9904	0.9869	0.9889	0.9887	0.9541

Table 4: R_b for girders in Table 1 with D/t_w =300 (t_w =0.183")

	Imperfection							Difference between Max and Min R_b
	Magnitude	1	2	3	4	5	6	
Girder 1	*D/67*	0.9091						0.0000
Girder 2	*D/ 67*	0.9352	0.9338	0.9332	0.9340	0.9385	0.9381	0.5761
Girder 3	*D/ 67*	0.9527	0.9397	0.9401	0.9594	0.9385	0.9560	2.2303
Girder 4	*D/ 67*	1.0047	1.0016	1.0029	0.9930	1.0029	1.0047	1.1870

From the above tables, it can be surmised that the limit loads are not sensitive to the base imperfection patterns or the magnitude of the web out-of-flatness. It is also observed that the normal stresses at the mid thickness of the web are not sensitive to the base imperfection pattern. Fig. 5 shows the normal stresses in the web at its mid thickness in Girder 4 for different imperfection patterns with a scale factor of 1/67. The lateral deflections in the web do not exhibit a consistent relationship to the base imperfection patterns. However, imperfection 2 is typically one of several imperfection patterns that produce higher web lateral deflections. Therefore, imperfection pattern 2 is chosen as the initial base imperfection seed to be used in all parametric studies discussed in this paper.

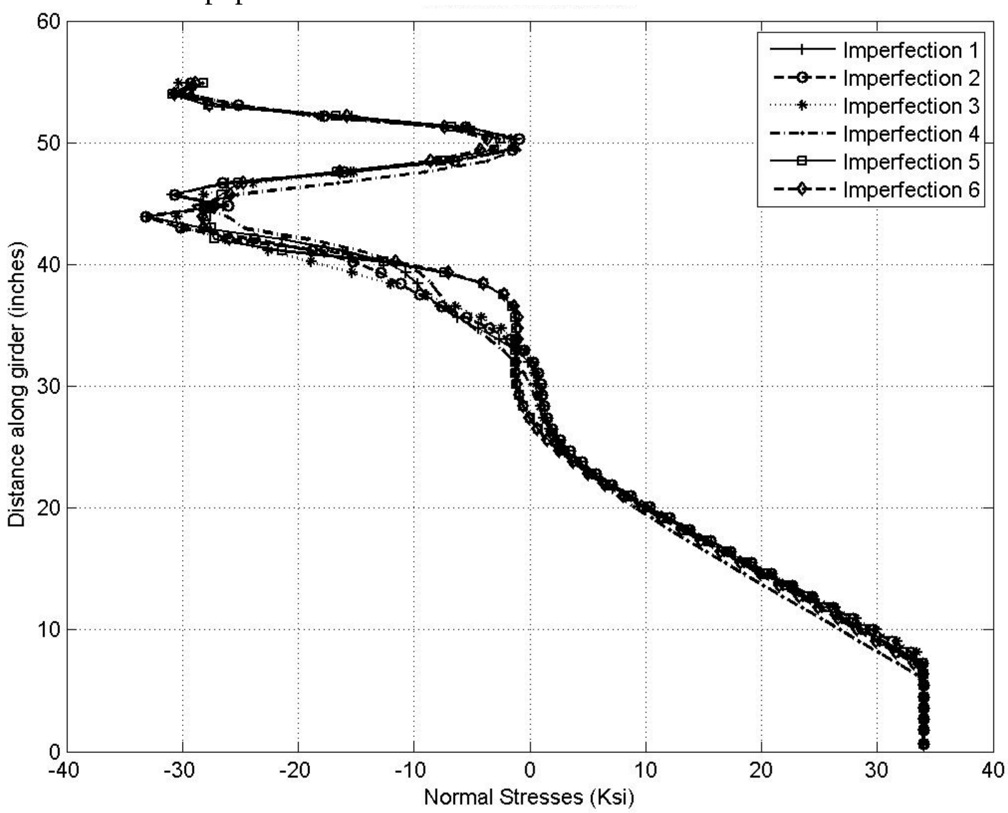

Figure 6: Normal stresses in web – Girder 4

4. Cases analyzed in parametric studies

Six cases, as defined in Table 5, are assessed as part of the parametric studies presented in this paper. Each case is defined by the aspect ratio (d_o/D) of its parametric studies. For instance Case 1 is a set of parametric studies for d_o/D = 1, with variable parameters such as D_c/D, D/t_w, and b_{fc}/D. The depth of the stiffener location is always at $0.4D_c$, which has generally been established as the theoretical optimum stiffener location. Cases 2, 3, and 4 are studies with d_o/D = 1.5, 2, and 0.75 respectively. The longitudinal stiffener sizes for each girder in each case are designed such that they are just sufficient to satisfy the corresponding AASHTO design criteria. A single size transverse stiffener is then used for all the analyses such that the minimum size requirement from AASHTO is satisfied for all the girders in all cases. The compression flanges of the test panels are braced such that LTB, according to the AASHTO LRFD provisions, does not govern any of the resistances in the studies presented in this paper. It must be noted that the rigidity requirement for the longitudinal stiffener in AASHTO is a function of d_o/D and thus the minimum rigidity of the longitudinal stiffener is greater for greater values of d_o/D. Thus, Cases and 3 employ longitudinal stiffeners of greater areas and rigidity than Case 1. In order to assess the importance of d_o/D as a parameter, Case 5 is designed such that the girders have a panel aspect ratio d_o/D = 1, but uses the same stiffener size as used in Case 2 (for d_o/D =2), thereby making every parameter for every girder in Cases 2 and 5 the same except for d_o/D. Similarly, Case 6 is designed such that every parameter for every girder in Cases 1 and 6 are the same except for the size of the longitudinal stiffener. The longitudinal stiffeners in Case 6 have a rigidity that is three times that of Case 1, while maintaining the AASHTO's minimum requirements on the b_l/t_l of the stiffener.

Table 5: Case definitions used in parametric studies

	d_o/D	Long Stiffener	Trans Stiffener	D_c/D	D/t_w	b_{fc}	d_s/D_c
Case 1	1	AASHTO min	AASHTO min	0.5,0.625,0.75	200, 240, 300	*D/6, D/5, D/4*	0.4
Case 2	1.5	AASHTO min	AASHTO min	0.5,0.625,0.75	200, 240, 300	*D/6, D/5, D/4*	0.4
Case 3	2	AASHTO min	AASHTO min	0.5,0.625,0.75	200, 240, 300	*D/6, D/5, D/4*	0.4
Case 4	0.75	AASHTO min	AASHTO min	0.5,0.625,0.75	200, 240, 300	*D/6, D/5, D/4*	0.4
Case 5	1	I-LS same as case 2	AASHTO min	0.5,0.625,0.75	200, 240, 300	*D/6, D/5, D/4*	0.4
Case 6	1	I-LS 3 times case1	AASHTO min	0.5,0.625,0.75	200, 240, 300	*D/6, D/5, D/4*	0.4

5. Results

The "true R_b" values are calculated from the test simulations as M_{max}/ M_y, where M_y is the girder yield moment determined by including the contribution of the longitudinal stiffener to the section modulus of the girder. The girders have nominal resistance of M_y if R_b = 1. The inclusion of the longitudinal stiffener in the girder moment of inertia (I_x) calculation increases the girder yield moment. It is found that the maximum R_b values from the test simulations are closer to 1.0 when the longitudinal stiffener is included in the calculation of the girder section modulus. Non-symmetry of the section due to eccentricity of the longitudinal stiffener is neglected.

Case 1 is analyzed twice, once with the residual stress distributions as discussed earlier and the second time omitting the residual stresses in the web. Table 6 shows a comparison of the values obtained from these two sets of analyses. The difference in the R_b values obtained is small (within 0.5 % for most cases). This suggests that the web residual stresses have a minor influence on the response. There are a few outliers that deserve further scrutiny in subsequent research. It is expected that these outliers are due to difficulties in the FEA continuation of the load-deflection responses causing some elastic unloading of several test girders before the actual limit load is reached. Therefore, the residual stresses in the web are neglected in the remaining studies.

Tables 7 and 8 provide R_b as obtained from the FEA test simulations for Cases 1 and 3 and compare these values with the corresponding resistance ratios estimated from current AASHTO and Eurocode (EN 1993-1-5) provisions. The tables show results obtained from FEA test simulations for girders with and without the longitudinal stiffeners. The complete set of results, along with the calculations from AASHTO and Eurocode are only presented for Cases 1 and 3. Other cases show similar trends in the values of R_b and in their relationship with the AASHTO and Eurocode estimations of "R_b." Table 9 shows values of R_b obtained for girders with longitudinal stiffeners (the main domain of interest), with cases arranged in increasing order of the longitudinal stiffener sizes.

Table 6: R_b values for Case 1 comparing analyses with full residual stresses and web residual stresses omitted

(a): D/t_w = 300

b_{fc}	*Dc/D*	W/RS	W/O RS	% DIFF	W/RS	W/O RS	% DIFF
		WITH LONG STIFFENER			NO LONG STIFFENER		
D/6	0.5000	0.9614	0.9545	0.7125	0.8497	0.4266	49.7900
D/6	0.6250	0.8802	0.8794	0.0879	0.7960	0.7941	0.2295
D/6	0.7500	0.8284	0.8316	-0.3857	0.7575	0.7547	0.3623
D/5	0.5000	0.9625	0.9580	0.4640	0.8726	0.8687	0.4535
D/5	0.6250	0.9067	0.9052	0.1674	0.8623	0.8388	2.7262
D/5	0.7500	0.8624	0.8622	0.0268	0.8123	0.8106	0.2020
D/4	0.5000	0.9790	0.9774	0.1682	0.9246	0.4079	55.8831
D/4	0.6250	0.9390	0.9382	0.0800	0.9150	0.9042	1.1802
D/4	0.7500	0.9080	0.9078	0.0275	0.8748	0.8737	0.1207

(b): D/t_w = 240

b_{fc}	*Dc/D*	W/RS	W/O RS	% DIFF	W/RS	W/O RS	% DIFF
		WITH LONG STIFFENER			NO LONG STIFFENER		
D/6	0.5000	1.0148	1.0150	-0.0199	0.8453	0.8415	0.4538
D/6	0.6250	0.9334	0.9308	0.2795	0.7912	0.7885	0.3491
D/6	0.7500	0.8601	0.8675	-0.8559	0.7493	0.7495	-0.0272
D/5	0.5000	1.0137	1.0139	-0.0239	0.8871	0.8810	0.6876
D/5	0.6250	0.9316	0.9455	-1.4873	0.8375	0.8347	0.3231
D/5	0.7500	0.8852	0.8830	0.2504	0.8029	0.8013	0.2009
D/4	0.5000	1.0142	1.0133	0.0849	0.9336	0.9216	1.2781
D/4	0.6250	0.9529	0.9529	0.0009	0.8927	0.8914	0.1531
D/4	0.7500	0.9152	0.9184	-0.3435	0.8648	0.8640	0.0907

(b): D/t_w = 200

b_{fc}	*Dc/D*	W/RS	W/O RS	% DIFF	W/RS	W/O RS	% DIFF
		WITH LONG STIFFENER			NO LONG STIFFENER		
D/6	0.5000	1.0316	1.0593	-2.6822	0.8589	0.8468	1.4182
D/6	0.6250	0.9971	1.0000	-0.2927	0.7888	0.7933	-0.5678
D/6	0.7500	0.9296	0.9367	-0.7619	0.7450	0.7489	-0.5237
D/5	0.5000	1.0598	1.0317	2.6480	0.8956	0.8872	0.9378
D/5	0.6250	0.9885	1.0003	-1.1978	0.8359	0.8389	-0.3685
D/5	0.7500	0.9333	0.9449	-1.2416	0.7950	0.7978	-0.3474
D/4	0.5000	1.0144	1.0408	-2.5993	0.9345	0.9288	0.6052
D/4	0.6250	0.9983	1.0041	-0.5883	0.8949	0.8934	0.1623
D/4	0.7500	0.9463	0.9556	-0.9805	0.8617	0.8621	-0.0493

Figures 7 and 8 show the variation of the lateral displacement of the web, relative to the initial imperfect geometry at the center of the test panel at the location of the longitudinal stiffener normalized with respect to the overall depth of the web (U/D) versus the applied load as a fraction of the test girder yield load P_y. In Figs. 7 and 8, P_y is calculated neglecting the contribution of longitudinal stiffener to the section modulus of the girder. This is done in order to observe the influence of the longitudinal stiffeners relative to a common reference load level.

Table 7: Comparison of R_b values for Case 1 from FEA, AASHTO and Eurocode

		D_c/D = 0.5								
		WITH LONGITUDINAL STIFFENER					NO LONGITUDINAL STIFFENER			
b_{fc}	D/t_w	$R_{bAASHTO}$	R_{bEC}	R_{bFEA}	$R_{bFEA}/R_{bAASHTO}$	R_{bFEA}/R_{bEC}	R_{bEC}	R_{bFEA}	$R_{bFEA}/R_{bAASHTO}$	R_{bFEA}/R_{bEC}
D/6	300	0.8192	0.8571	0.9545	1.1652	1.1137	0.7767	0.8497	1.0372	1.0940
	240	0.8683	0.8712	1.0150	1.1690	1.1651	0.7517	0.8415	0.9691	1.1194
	200	0.9104	0.8959	1.0593	1.1635	1.1824	0.7368	0.8468	0.9301	1.1492
D/5	300	0.8573	0.8879	0.9580	1.1176	1.0789	0.8280	0.8687	1.0133	1.0491
	240	0.8943	0.8976	1.0139	1.1337	1.1295	0.8058	0.8810	0.9852	1.0934
	200	0.9271	0.9166	1.0317	1.1129	1.1255	0.7913	0.8872	0.9570	1.1212
D/4	300	0.9014	0.9232	0.9774	1.0843	1.0587	0.8848	0.9246	1.0258	1.0450
	240	0.9256	0.9287	1.0133	1.0948	1.0911	0.8676	0.9216	0.9958	1.0623
	200	0.9477	0.9413	1.0408	1.0982	1.1057	0.8555	0.9288	0.9800	1.0857

		D_c/D = 0.625								
		WITH LONGITUDINAL STIFFENER					NO LONGITUDINAL STIFFENER			
b_{fc}	D/t_w	$R_{bAASHTO}$	R_{bEC}	R_{bFEA}	$R_{bFEA}/R_{bAASHTO}$	R_{bFEA}/R_{bEC}	R_{bEC}	R_{bFEA}	$R_{bFEA}/R_{bAASHTO}$	R_{bFEA}/R_{bEC}
D/6	300	0.6952	0.8055	0.8794	1.2650	1.0917	0.7211	0.7941	1.1423	1.1012
	240	0.7620	0.8147	0.9308	1.2215	1.1425	0.6911	0.7885	1.0347	1.1409
	200	0.8182	0.8370	1.0000	1.2222	1.1947	0.6719	0.7933	0.9696	1.1808
D/5	300	0.7554	0.8448	0.9052	1.1984	1.0716	0.7807	0.8388	1.1104	1.0745
	240	0.8057	0.8493	0.9455	1.1735	1.1132	0.7528	0.8348	1.0361	1.1089
	200	0.8492	0.8653	1.0003	1.1779	1.1560	0.7333	0.8389	0.9879	1.1440
D/4	300	0.8277	0.8915	0.9382	1.1335	1.0524	0.8494	0.9042	1.0924	1.0644
	240	0.8602	0.8922	0.9529	1.1078	1.0680	0.8268	0.8914	1.0362	1.0781
	200	0.8895	0.9016	1.0041	1.1289	1.1137	0.8096	0.8934	1.0044	1.1035

		D_c/D = 0.75								
		WITH LONGITUDINAL STIFFENER					NO LONGITUDINAL STIFFENER			
b_{fc}	D/t_w	$R_{bAASHTO}$	R_{bEC}	R_{bFEA}	$R_{bFEA}/R_{bAASHTO}$	R_{bFEA}/R_{bEC}	R_{bEC}	R_{bFEA}	$R_{bFEA}/R_{bAASHTO}$	R_{bFEA}/R_{bEC}
D/6	300	0.5532	0.7617	0.8316	1.5032	1.0917	0.6827	0.7547	1.3643	1.1055
	240	0.6408	0.7643	0.8675	1.3538	1.1349	0.6480	0.7494	1.1696	1.1564
	200	0.7127	0.7815	0.9367	1.3142	1.1986	0.6243	0.7489	1.0507	1.1995
D/5	300	0.6363	0.8087	0.8622	1.3550	1.0662	0.7478	0.8106	1.2739	1.0840
	240	0.7022	0.8072	0.8830	1.2574	1.0939	0.7153	0.8013	1.1411	1.1203
	200	0.7583	0.8183	0.9449	1.2461	1.1548	0.6914	0.7978	1.0520	1.1538
D/4	300	0.7394	0.8652	0.9078	1.2277	1.0492	0.8246	0.8737	1.1817	1.0595
	240	0.7816	0.8610	0.9184	1.1750	1.0667	0.7978	0.8640	1.1055	1.0830
	200	0.8192	0.8661	0.9556	1.1666	1.1033	0.7766	0.8621	1.0524	1.1100

Table 8: Comparison of R_b values for Case 3 from FEA, AASHTO and Eurocode

		D_c/D = 0.5								
		WITH LONGITUDINAL STIFFENER					NO LONGITUDINAL STIFFENER			
b_{fc}	D/t_w	$R_{b\mathrm{AASHTO}}$	$R_{b\mathrm{EC}}$	$\mathrm{R_{bFEA}}$	$R_{b\mathrm{FEA}}/R_{b\mathrm{AASHTO}}$	$R_{b\mathrm{FEA}}/R_{b\mathrm{EC}}$	$R_{b\mathrm{EC}}$	$R_{b\mathrm{FEA}}$	$R_{b\mathrm{FEA}}/R_{b\mathrm{AASHTO}}$	$R_{b\mathrm{FEA}}/R_{b\mathrm{EC}}$
D/6	300	0.8192	0.8571	0.9987	1.2191	1.1653	0.7767	0.8240	1.0059	1.0609
	240	0.8683	0.8765	0.9895	1.1396	1.1290	0.7517	0.8294	0.9552	1.1034
	200	0.9104	0.9030	1.0785	1.1847	1.1943	0.7368	0.8180	0.8986	1.1102
D/5	300	0.8573	0.8867	1.0042	1.1714	1.1325	0.8280	0.8677	1.0122	1.0480
	240	0.8943	0.9005	1.0369	1.1594	1.1514	0.8058	0.8816	0.9858	1.0941
	200	0.9271	0.9212	1.0045	1.0835	1.0904	0.7913	0.8632	0.9311	1.0908
D/4	300	0.9014	0.9212	1.0066	1.1168	1.0928	0.8848	0.9284	1.0300	1.0493
	240	0.9256	0.9294	0.9946	1.0746	1.0701	0.8676	0.9239	0.9982	1.0649
	200	0.9477	0.9434	1.0450	1.1026	1.1077	0.8555	0.9320	0.9834	1.0895

		D_c/D = 0.625								
		WITH LONGITUDINAL STIFFENER					NO LONGITUDINAL STIFFENER			
b_{fc}	D/t_w	$R_{b\mathrm{AASHTO}}$	$R_{b\mathrm{EC}}$	$\mathrm{R_{bFEA}}$	$R_{b\mathrm{FEA}}/R_{b\mathrm{AASHTO}}$	$R_{b\mathrm{FEA}}/R_{b\mathrm{EC}}$	$R_{b\mathrm{EC}}$	$R_{b\mathrm{FEA}}$	$R_{b\mathrm{FEA}}/R_{b\mathrm{AASHTO}}$	$R_{b\mathrm{FEA}}/R_{b\mathrm{EC}}$
D/6	300	0.6952	0.8042	0.9609	1.3823	1.1949	0.7211	0.7780	1.1192	1.0789
	240	0.7620	0.8194	1.0077	1.3224	1.2298	0.6911	0.7555	0.9914	1.0932
	200	0.8182	0.8441	1.0526	1.2865	1.2471	0.6719	0.7532	0.9206	1.1211
D/5	300	0.7554	0.8424	0.9801	1.2975	1.1635	0.7807	0.8439	1.1172	1.0810
	240	0.8057	0.8517	1.0169	1.2622	1.1940	0.7528	0.8149	1.0115	1.0825
	200	0.8492	0.8697	1.0470	1.2328	1.2038	0.7333	0.8094	0.9531	1.1037
D/4	300	0.8277	0.8886	0.9908	1.1970	1.1151	0.8494	0.8966	1.0832	1.0555
	240	0.8602	0.8924	1.0121	1.1766	1.1341	0.8268	0.8763	1.0187	1.0598
	200	0.8895	0.9034	1.0423	1.1718	1.1537	0.8096	0.8747	0.9834	1.0804

		D_c/D = 0.75								
		WITH LONGITUDINAL STIFFENER					NO LONGITUDINAL STIFFENER			
b_{fc}	D/t_w	$R_{b\mathrm{AASHTO}}$	$R_{b\mathrm{EC}}$	$\mathrm{R_{bFEA}}$	$R_{b\mathrm{FEA}}/R_{b\mathrm{AASHTO}}$	$R_{b\mathrm{FEA}}/R_{b\mathrm{EC}}$	$R_{b\mathrm{EC}}$	$R_{b\mathrm{FEA}}$	$R_{b\mathrm{FEA}}/R_{b\mathrm{AASHTO}}$	$R_{b\mathrm{FEA}}/R_{b\mathrm{EC}}$
D/6	300	0.5532	0.7600	0.8897	1.6082	1.1706	0.6827	0.7441	1.3450	1.0899
	240	0.6408	0.7691	0.9498	1.4823	1.2350	0.6480	0.7262	1.1333	1.1206
	200	0.7127	0.7891	1.0001	1.4032	1.2674	0.6243	0.7127	1.0000	1.1416
D/5	300	0.6363	0.8059	0.9091	1.4287	1.1281	0.7478	0.8013	1.2593	1.0716
	240	0.7022	0.8094	0.9640	1.3729	1.1910	0.7153	0.8000	1.1393	1.1185
	200	0.7583	0.8230	0.9957	1.3131	1.2099	0.6914	0.7731	1.0195	1.1181
D/4	300	0.7394	0.8620	0.9334	1.2624	1.0829	0.8246	0.8670	1.1726	1.0514
	240	0.7816	0.8610	0.9774	1.2506	1.1352	0.7978	0.8648	1.1065	1.0840
	200	0.8192	0.8680	1.0086	1.2312	1.1620	0.7766	0.8440	1.0303	1.0868

Table 9: Comparison of R_b values for all cases

(a) D/t_w = 300

	b_l/t_l	A_l	I_l	D_c/D =0.5, b_{fc}= $D/6$	D_c/D= 0.625, b_{fc}= $D/6$	D_c/D= 0.75, b_{fc}= $D/6$	D_c/D =0.5, b_{fc}= $D/5$	D_c/D= 0.625, b_{fc}= $D/5$	D_c/D= 0.75, b_{fc}= $D/5$	D_c/D= 0.5, b_{fc}= $D/4$	D_c/D= 0.625, b_{fc}= $D/4$	D_c/D= 0.75, b_{fc}= $D/4$
Case4	11.55	2.77	23.78	0.93	0.87	0.82	0.95	0.89	0.86	0.97	0.93	0.90
Case1	11.20	4.38	49.15	0.95	0.88	0.83	0.96	0.91	0.86	0.98	0.94	0.91
Case2	11.56	6.85	105.33	0.99	0.92	0.89	1.00	0.94	0.90	1.01	0.96	1.02
Case5	11.56	6.85	105.33	1.01	0.95	0.90	1.01	0.96	0.93	1.01	0.97	0.95
Case6	11.56	7.72	127.70	1.01	0.97	0.92	1.01	0.98	0.94	1.01	0.99	0.96
Case3	11.55	9.56	180.87	1.00	0.96	0.89	1.00	0.98	0.91	1.01	0.99	0.93

(b) D/t_w = 240

	b_l/t_l	A_l	I_l	D_c/D =0.5, b_{fc}=D $/6$	D_c/D= 0.625, b_{fc}= $D/6$	D_c/D= 0.75, b_{fc}= $D/6$	D_c/D =0.5, b_{fc}= $D/5$	D_c/D= 0.625, b_{fc}= $D/5$	D_c/D= 0.75, b_{fc}= $D/5$	D_c/D =0.5, b_{fc}= $D/4$	D_c/D= 0.625, b_{fc}= $D/4$	D_c/D= 0.75, b_{fc}= $D/4$
Case4	11.54	3.75	45.50	0.98	0.90	0.84	0.99	0.92	0.87	0.99	0.94	0.91
Case1	11.43	5.60	88.07	1.02	0.93	0.87	1.01	0.95	0.88	1.01	0.95	0.92
Case2	11.46	9.08	195.01	1.04	0.98	0.93	1.03	1.00	0.95	1.01	1.01	0.97
Case5	11.46	9.08	195.01	1.05	1.01	0.94	1.04	1.01	0.96	1.03	1.01	0.97
Case6	11.55	10.51	249.46	1.03	1.02	0.96	1.00	1.01	0.97	1.03	1.02	0.98
Case3	11.56	12.99	351.64	0.99	1.01	0.95	1.04	1.02	0.96	0.99	1.01	0.98

(c) D/t_w = 200

	b_l/t_l	A_l	I_l	D_c/D =0.5, b_{fc}= $D/6$	D_c/D= 0.625, b_{fc}= $D/6$	D_c/D= 0.75, b_{fc}= $D/6$	D_c/D =0.5, b_{fc}= $D/5$	D_c/D= 0.625, b_{fc}= $D/5$	D_c/D= 0.75, b_{fc}= $D/5$	D_c/D =0.5, b_{fc}= $D/4$	D_c/D= 0.625, b_{fc}= $D/4$	D_c/D= 0.75, b_{fc}= $D/4$
Case4	11.54	4.88	79.32	1.04	0.96	0.90	1.03	0.97	0.91	1.02	0.98	0.93
Case1	11.25	7.20	149.08	1.06	1.00	0.94	1.03	1.00	0.94	1.04	1.00	0.96
Case2	11.45	11.68	335.93	1.08	1.03	0.97	1.02	1.03	0.98	1.01	1.03	1.00
Case5	11.45	11.68	335.93	1.02	1.04	0.99	1.01	1.05	0.99	1.05	1.04	1.00
Case6	11.55	13.53	430.72	1.09	1.06	1.00	1.06	1.06	1.01	1.05	1.05	1.01
Case3	11.56	16.64	603.70	1.08	1.05	1.00	1.00	1.05	1.00	1.05	1.04	1.01

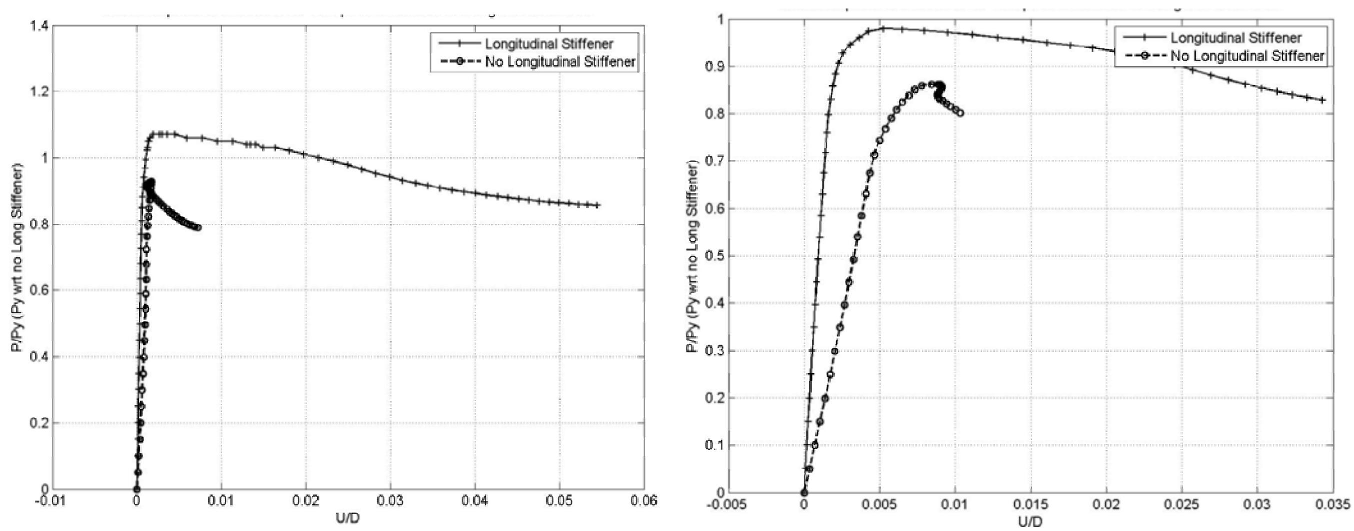

(D_c/D = 0.5, b_{fc} = $D/4$

(D_c/D = 0.75, b_{fc} = $D/4$

Figure 7: Normalized lateral displacement at Location of Longitudinal Stiffener for D/t_w = 200 (Case1)

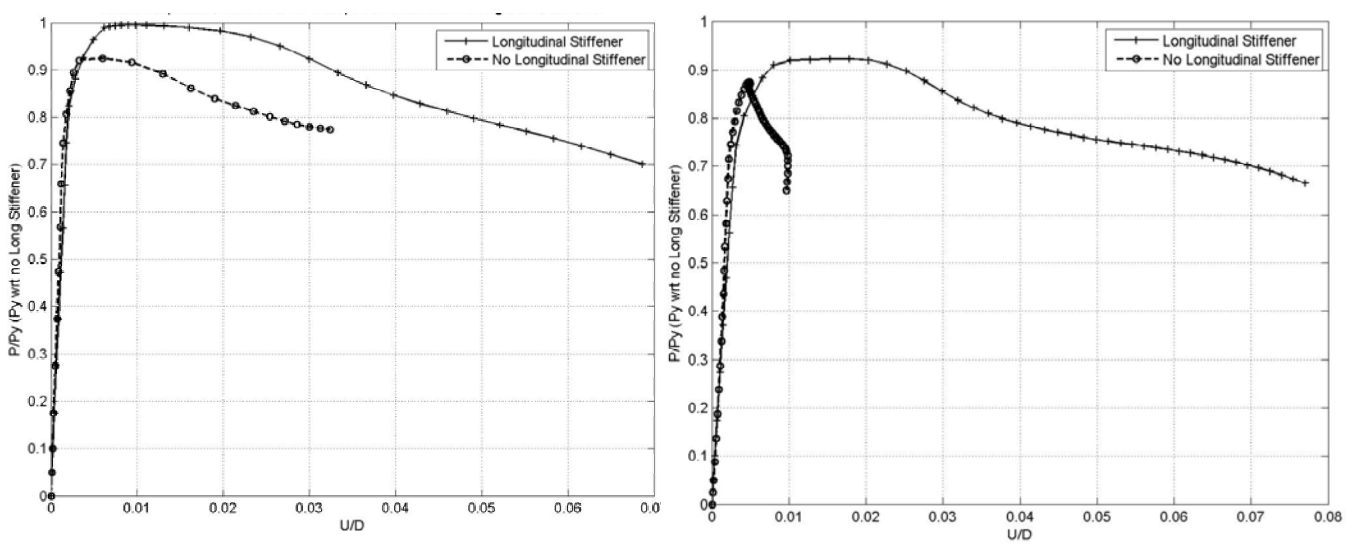

(D_c/D = 0.5, b_{fc} = $D/4$

(D_c/D = 0.75, b_{fc} = $D/4$

Figure 8: Normalized lateral displacement at Location of Longitudinal Stiffener for D/t_w = 300(Case1)

6. Observations and Conclusions

1. It is clear that including a longitudinal stiffener always provides an improvement in the flexural resistance of the girder as compared to girders without longitudinal stiffeners, although theoretically, the minimum size longitudinal stiffeners from AASHTO LRFD are not generally sufficient to develop the maximum potential bend post-buckling capacity of the girders.
2. Increasing the ratio of D_c/D or decreasing the ratio A_{fc}/A_{wc} results in a reduction in R_b as per the AASHTO LRFD design equations. This is also the case with the FEA test simulations. The behavior is more pronounced for more slender webs. However, AASHTO under predicts the true R_b (as determined by simulations) significantly for higher D_c/D (9 to 50%). The parameter R_b calculated as per AASHTO (neglecting any contribution from the longitudinal stiffener) is conservative even in the absence of a longitudinal stiffener as seen in Tables 7 and 8 for high D_c/D ratios of 0.75. This is due to the fact that the original derivation of R_b by Basler and Thurliman is based only on a single very idealized extreme girder geometry (Salmon et al. 2009). The prediction by AASHTO improves for higher values of b_{fc}/D ratios.
3. It is observed that the effect of b_{fc}/D is less substantial than the effect of D_c/D. Both of these variables influence the ratio A_{fc}/A_{wc} which then has an influence on R_b. However, there are also other complex characteristics that are influenced by changing these parameters.
3. In Table 9, the difference in values of R_b between Cases 2 and 5 is negligible (1 to 2 %). The only difference between these two cases is the d_o/D (see Table 5). The two cases use the same girder dimensions and stiffener dimensions. While the stiffener size used in the two cases is the minimum as required for Case 2, it is much higher than the minimum requirements as per AASHTO for Case 5 ($d_o/D = 1$). This indicates that d_o/D plays a small role in influencing the R_b value. This is an expected result.
4. In Table 9, one can observe that as the size of the longitudinal stiffener is increased, a higher value of R_b is obtained. However, it is also evident that beyond a certain size of the longitudinal stiffener, no significant increase in R_b is obtained. That is, the “law of diminishing returns” applies.
5. The exact role of the longitudinal stiffener in contributing to the strength of the girder is still under study, but from Figs. 7 and 8, it may be observed that the longitudinal stiffener provides better restraint to the web lateral deflection than the girders with no longitudinal stiffening for D/t_w of 200. For the more slender webs with D/t_w of 300, the longitudinal stiffener does not appear to provide any significant improvement. The longitudinal stiffeners sized as per minimum AASHTO requirements perform better in terms of restraining the web lateral displacement for less slender webs than they do for more slender webs.
6. The increase in R_b when the size of the longitudinal stiffener is increased to three times the minimum required lateral rigidity as per AASHTO only gives an increase of about 5 to 7 % in the R_b value. The R_b obtained for stiffeners with three times the minimum lateral rigidity is not significantly higher than for stiffeners with about twice the minimum lateral rigidity. This is an indication that, while it may be beneficial to increase the stiffener rigidity to some extent from the current AASHTO minimum requirements, there are diminishing returns as the stiffener size is made larger and larger. It is noteworthy, however, that significant improvements over the current AASHTO provisions, which completely neglect the contribution of the longitudinal stiffener to the flexural resistance of the girder in the post buckling range of the response, may be obtained in determining a “true R_b” even using the current AASHTO requirements for the minimum size of the longitudinal stiffener.

7. The Eurocode calculations are closer to the FEA test simulations, but are also on the conservative side. These calculations are conceptually more rigorous, and more elaborate, and take into account the stress states in the web and the stiffener in calculating the plate buckling resistance using cross section effective plate widths. For the cases presented in this paper, the Eurocode predicts lower R_b values for *smaller* web slenderness ratios in girders with no longitudinal stiffening. This can be explained physically by the fact that girders with lower slenderness ratios in the current study have the same overall web panel panel depth, but thicker web plates, and hence have greater moments of inertia than the girders with higher slenderness ratios. This increases the value of M_y, which brings down the values of R_b while calculating an effective cross section in the post buckling range.

7. Future Work

1. The work in this paper is restricted to an optimum depth of the stiffener (0.4 D_c). The influence of the location of the stiffener depth is currently under study.
2. The work in this paper precludes the occurrence of LTB or local buckling in the compression flange. In order to make this study more complete, the authors will assess the influence of coupled buckling modes by including the effects of lateral torsional buckling and flange local buckling. This more complete study will be used to develop recommendations for modifying current AASHTO provisions to better account for the size of the longitudinal stiffeners and D_c/D in the calculation of R_b.
3. The work in this paper will be extended to study the effects of high shear on test panels and to ensure that any suggested recommendations perform satisfactorily under high shear conditions.
4. Similar studies will be performed on girders with horizontal curvature.

References

AASHTO. 2007. AASHTO LRFD Bridge Design Specifications. 5th Edition, American Association of State Highway and Transportation Officials, Washington, DC. U.S. customary and metric editions.

AWS (2010). Structural Welding Code–Steel, AWS D1.1: D1.1M, 22nd ed., prepared by AWS Committee on Structural Welding, 572 pp.

Basler, K., and B. Thurlimann. (1961). “Strength of Plate Girders in Bending.” Journal of the Structural Division, American Society of Civil Engineers, New York, NY, Vol. 87, No. ST6, August 1961, pp. 153–181.

Cooper, P.B (1965). “Bending and Shear Strength of Longitudinally Stiffened Plate Girders,” Fritz. Eng .Lab.Rep.No.304.6, Lehigh University, Bethlehem, PA, Sept

Cooper, P.B (1967). “Strength of Longitudinally Stiffened Plate Girders”, ASCE J. Struct. Div., Vol. 93, No. ST2, pp.419-452.

Cooper, P.B (1971). “The Ultimate Bending Moment for Plate Girders”, paper presented at the IABSE Colloq. Des. Plate Box Girders Ultimate Strength, London.

Dubas, C. (1948) “A Contribution to the Buckling of Stiffened Plates,” IABSE Preliminary Publication. Third Congress, International Association for Bridge and Structural Engineers, Zurich, Switzerland.

CEN (2006), Eurocode 3: Design of Steel Structures, Part 1-5:General Rules - Plated Structural Elements, EN 1993-1-5:2006: E, Incorporating Corrigendum April 2009, European Committee for Standardization, Brussels, Belgium, 56 pp.

Frank, K. H., and Helwig, T. A. (1995), “Buckling od Webs in Unsymmetric Plate Girders,” AISC Eng. J., Vol.32, No. 2, pp.43-53.

Fukumoto, Y., and Kubo, M. (1977) “A Supplement of a Survey of Tests on Lateral Buckling Strength of Beam,” ECCS. Final Report, Second International Colloquium on Stability of Steel Structures, Liége, Belgium, pp. 115–117.

Fukumoto, Y., and Kubo, M. (1977) “An Experimental Review of Lateral Buckling of Beams and Girders,” International Colloquium on Stability of Steel Structures under Static and Dynamic Load, American Society of Civil Engineers (2nd edn.) , pp. 541-562

Fukumoto, Y., and Kubo, M. (1972) “Lateral Buckling Strength of Girders with Bracing Systems,” Preliminary Rep. 9th Cong. IABSE (2nd edn.), pp 299-304, Amsterdam.

Hoglund, T. (1981) “Design of Thin Plate I Girders in Shear and Bending, with Special Reference to Web Buckling,” Bulletin No. 94, Division of Building Statics and Structural Engineering, Royal Institute of Technology, Stockholm.

Hoglund, T. (1995) “Strength of Steel and Aluminum Plate Girders – Shear buckling and Overall Web buckling of Plane and trapezoidal Webs. Comparison with Tests,” Department of Structural Engineering, Royal Institute of Technology, Stockholm, technical Report 1995:4 Steel Structures.

Johansson, B., and Veljkovic, M. (2001), “Steel Plated Structures,” Lulea University of Technology, Sweden.

Johansson, B., Maquoi, R. and Sedlacek, G. (2001), “New Design Rules for Plated Structures in Eurocode 3,” Journal of Construction Steel Research, 57, 279-311.

Johansson, B., Maquoi, R., Sedlacek, G., Muller, C. and Beg, D. (2007), “Commentary and Worked Examples to EN 1993-1-5 “Plated Structural Elements”,” JRC Scientific and Technical Reports.

Laane, A. (2003) “Post Critical Behavior of Composite Bridges under Negative Moment and Shear,” Thesis No. 2889, EPFL, Lausanne.

Massonnet, C. (1960) “Stability Considerations in the Design of Steel Plate Girders,” Journal of the Structural Division, American Society of Civil Engineers, No 2350 (ST1), 71-97

Prawel, S.P., Morrell, M.L. and Lee, G.C. (1974), “Bending and Buckling Strength of Tapered Structural Members,” Welding Research Supplement, Vol. 53, February, 75-84.

Salmon, C.G. and Johnson, J.E. (2009), *Steel Structures, Design and Behavior*, 5th Ed., Prentice Hall, NJ, 866 pp.

Simulia (2013), ABAQUS/Standard Version 6.12-1, Simulia, Inc. Providence, RI.

Veljkovic, M., and Johansson, B. (2001), “Design for Buckling of Plates due to Direct Stress,” Proceedings of Nordic Steel Construction Conference, Helsinki.

Ziemian, R., (2010), “Guide to stability Design Criteria for Metal Structures,” 6th Edition